Auxiliary material for Paper 2008GL036865

Seismic evidence for thermally□controlled dehydration reaction in subducting oceanic crust

Junichi Nakajima□ Yusuke Tsuji□ and Akira Hasegawa
Research Center for Prediction of Earthquakes and Volcanic Eruptions□ Graduate School of Science□ Tohoku University□ Sendai□ Japan

Nakajima□ J□□ Y□ Tsuji□ and A□ Hasegawa □2009□□ Seismic evidence for thermally□ controlled dehydration reaction in subducting oceanic crust□ Geophys□ Res□ Lett□□ 36□ L03303□ doi□10□1029□2008GL036865□

Introduction

This dataset contains two text files□ which describes the data and method of tomographic inversions and detailed method of checkerboard resolution tests□ and three figures□ an initial velocity model used in the inversion □Figure S1□□ results of checkerboard resolution tests and a semblance□based statistic from checkerboard tests for S wave □Figure S2□□ and results of P□wave velocity structures and checkerboard resolution tests □Figure S3□□

1□ 2008gl036865□txts01□txt
Data and Methods of the tomographic inversions□

2□ 2008gl036865□txts02□txt
Methods of resolution tests□

3□ 2008gl036865□fs01□jpg
Initial velocity model□ P□ and S□wave initial velocity models used in the inversion□

4□ 2008gl036865□fs02□jpg
Results of checkerboard resolution tests for S wave□ □a□ □Left□ Results of checkerboard resolution tests and □right□ semblance□based statistic □resolvability□ from checkerboard tests □Zelt□ 1998□ along lines □a□ A□A□ □ □b□ B□B□ □ and □c□ C□C□ shown in Figure 2□a□ in the manuscript□ Black curves denote the upper surface of the Pacific slab□ Contours with derivative weighted sum □DWS□ □Thurber and Eberhart□Philipps□ 1999□ of 500 are shown by black dashed lines□

5□ 2008gl036865□fs03□jpg
Results of P□wave velocity structures and checkerboard resolution tests□ Across□ arc vertical cross sections of □left□ P□wave velocities and □right□ results of checkerboard resolution tests along lines □a□ A□A□ □ □b□ B□B□ □ and □c□ C□C□ shown in Figure 2□a□ in the manuscript□ Areas with values of DWS of □500 are shaded in P□wave velocities□ and contours with DWS□500 are shown by gray lines in checkerboard resolution tests□ Other symbols are the same as those in Figure 3□a□ in the manuscript□

References

Thurber□ C□ H□□ and D□ Eberhart□Phillips □1999□□ Local earthquake tomography with flexible gridding□ Comput□ Geosci□□ 25□ 809□818□

Zelt□ C□ A□ □1998□□ Lateral velocity resolution from three□dimensional seismic refraction data□ Geophys□ J□ Int□□ 135□ 1101□1112□

Text S1.

! n this study, we applied double-difference tomography method (Zhang and Thurber, 2003, 2006) to a large number of arrival-time data. Due to limitations on computational time and memory, the region was divided into four sub-regions and the computations were performed separately for each region (regions 1 to 4 in Figure 2 in the manuscript). The lateral extent of each region is 240 km × 200 km with a depth range of 0-200 km. We first selected earthquakes (M≥2.5) at depths of 0-40 km and those (M≥1.0) at deeper depths in the period between 2001 and 2007 from the unified catalogue of the Japan Metrological Agency. Then, only the earthquakes that satisfy the following condition were selected: Hdep≤Dmin, where Hdep is a depth of earthquake and Dmin is an epicentral distance to the nearest station with P- and S-wave arrival pickings. This criterion keeps earthquakes whose depth can be well constrained. We further added arrival-time data of earthquakes (depth > 100 km) that occurred from October 1997 to June 1999 to the data sets in sub-regions 1 and 2 to improve the resolution at the deeper part of the Pacific slab. These data were recorded at permanent stations and temporary ones conducted as a part of 1997-1999 Joint Seismological Observations Project by Japanese university groups (Hasegawa and Hirata, 1999). The numbers of earthquakes derived from that observation are 352 and 273 for sub-regions 1 and 2, respectively. It is noted that tomoFDD (Zhang and Thurber, 2006) is adopted in this study, which uses a finite-difference travel-time algorithm taking the curvature of the earth into consideration, because a lateral extent of the study area is 240 km × 200 km and hence the curvature of the Earth is not negligible. The final results were obtained after 12 iterations. The data sets used in this study are summarized in Table 1 in the manuscript.

References

Hasegawa, A., and N. Hirata (1999), Summary: Transect of the northeastern Japan arc - arc deformation and crustal activity- (in Japanese), Earth Mon., , 27, 5-11.

Zhang, H., and C. H. Thurber (2003), Double-Difference Tomography: The method and its application to the Hayward fault, California, Bull. Seismol. Soc. Am., 93, 1875-1889.

Zhang, H., and C. H. Thurber (2006), Development and applications of double-difference seismic tomography, Pure Appl. Geophys., 163, 373-403

Zhang, H., C. H. Thurber, D. Shelly, S. Ide, G. C. Beroza, and A. Hasegawa (2004), High-resolution subducting-slab structure beneath northern Honshu, Japan, revealed by double-difference tomography, Geology, 32, 361-364.

Text S2.

To ascertain the adequacy of ray coverage and reliability of obtained images, we carried out checkerboard resolution tests (CRTs) and the reconstruction tests (RTs) specialized for the low-velocity oceanic crust. In the CRTs positive and negative velocity perturbations of 10 % were assigned alternately to one grid node for the horizontal direction and two grid nodes for the vertical direction, and travel times for this model were calculated to generate synthetic data. Synthetic data were constructed from the same source-receiver geometry as the observations with random noises corresponding to picking errors (a standard deviation of 0.1 s for P wave and 0.15 s for S wave). Then we inverted the synthetic travel-time data thus calculated using an initial model without any velocity anomalies. If the checkerboard pattern is recovered well, we consider that the data is sufficient to resolve velocity anomalies comparable to the lateral extent of one grid node.

We also calculated the semblance between the exact and recovered checkerboard anomalies (resolvability) to assess the recovered checkerboard models quantitatively (Zelt, 1998). Zelt (1998) suggested that a semblance values of ≥0.7 provides a reliable indicator of where the recovered model closely resembles the true model based on empirical testing.

Figure S2 shows results of checkerboard tests and its resolvability with derivative weighted sum (DWS) (Thurber and Eberhart-Philipps, 1999) of 500. It is apparent that the regions with values of DWS of ≥500 can correspond to those in the Pacific slab where checkerboard patterns are relatively recovered and semblance values are larger than 0.7, even though regions with DWS≥500 do not have good recovery of checkerboard patters in the mantle wedge. Therefore, we use contours of DWS of ≥500 as a simple indicator to show well-resolved regions in the model space, and the regions with DWS ≥ 500 are shaded by white in Figures 3, 4, S2, and S3.

References

Thurber, C. H., and D. Eberhart-Phillips (1999), Local earthquake tomography with flexible gridding, Comput. Geosci., 25, 809-818.

Zelt, C. A. (1998), Lateral velocity resolution from three-dimensional seismic refraction data, Geophys. J. Int., 135, 1101-1112.

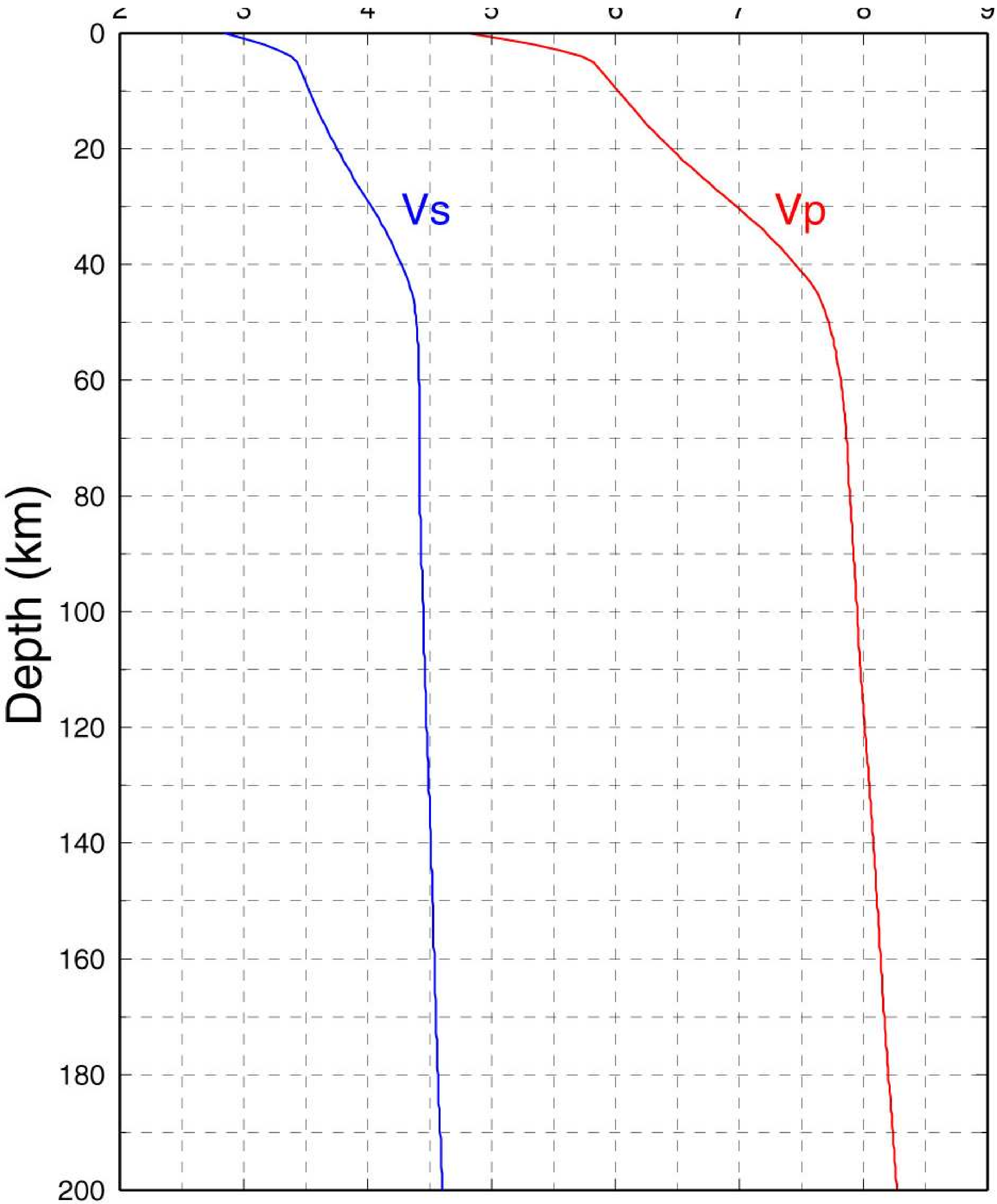
2
3
4
5
6
7
8
9
0
20
40
60
80
100
120
140
160
180
200
Depth (km)
Vs
Vp

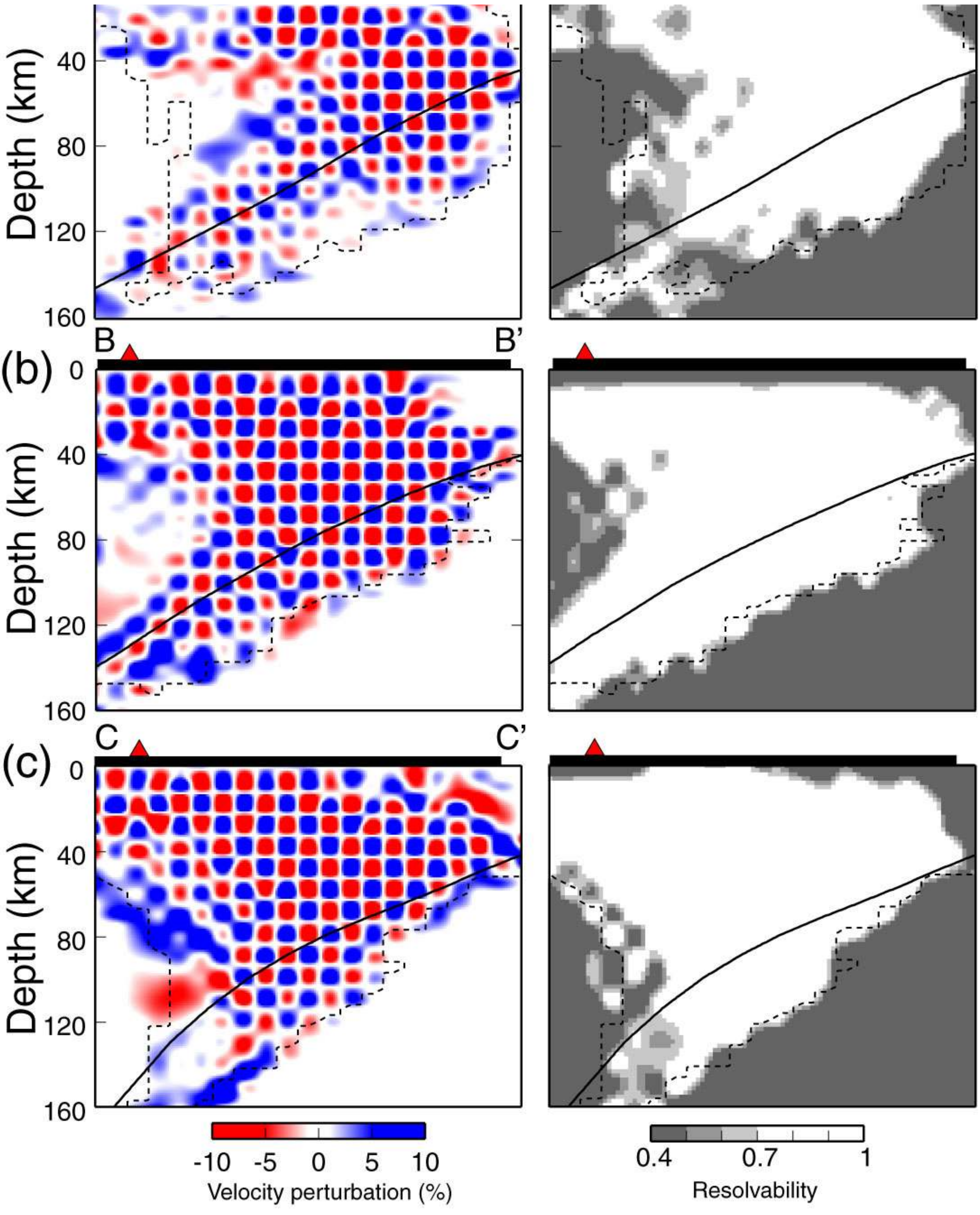

Depth (km)
40
80
120
160
B
B'
(b)
0
C
C'
(c)
-10 -5 0 5 10
Velocity perturbation (%)
0.4 0.7 1
Resolvability

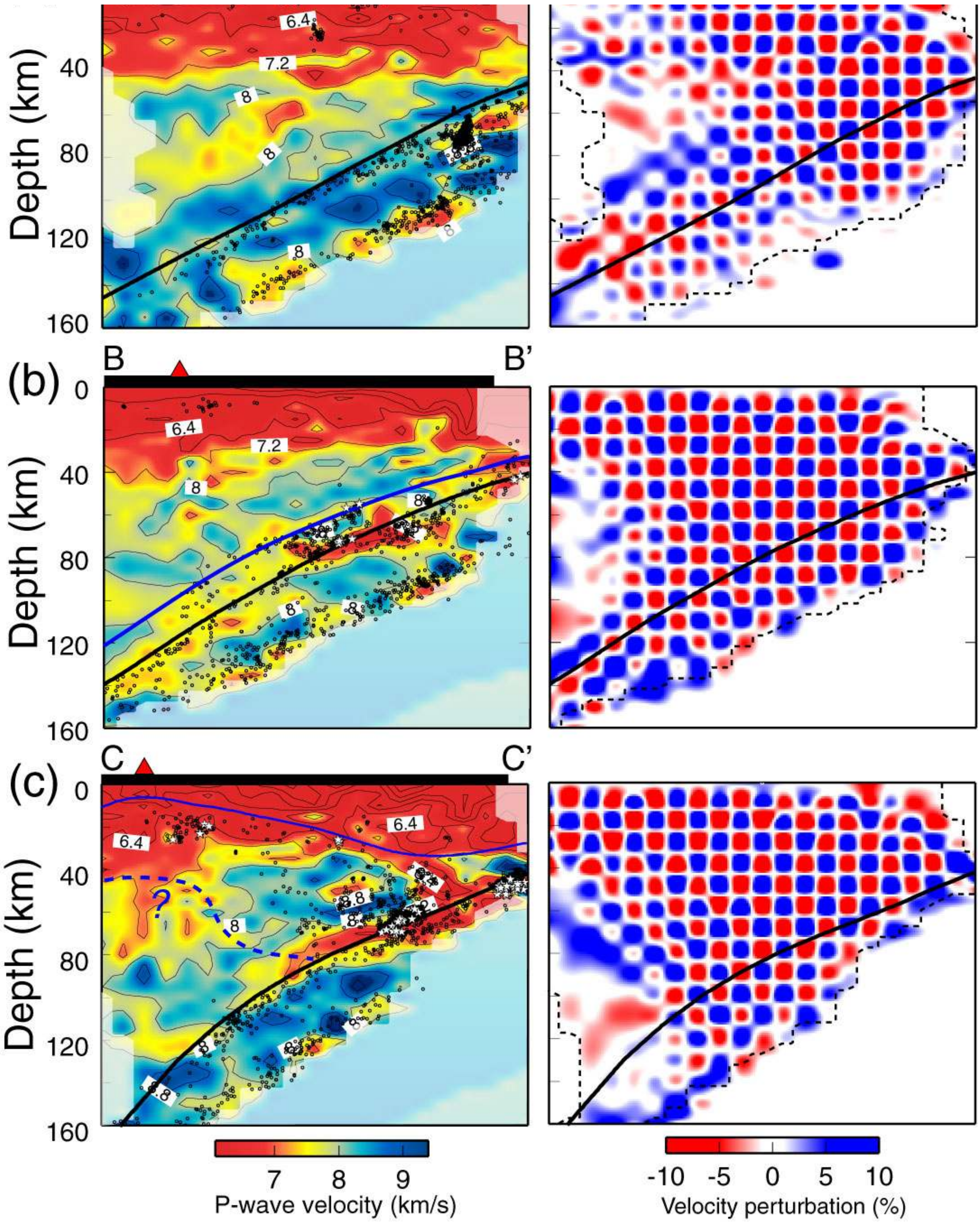

B
B'
(b)
C
C'
(c)
Depth (km)
0
40
80
120
160
6.4
7.2
8
?
7
8
9
P-wave velocity (km/s)
-10
-5
0
5
10
Velocity perturbation (%)